

Precise measurement of the  $CP$  violation parameter  $\sin 2\phi_1$  in  $B^0 \rightarrow (c\bar{c})K^0$  decays

I. Adachi,<sup>9</sup> H. Aihara,<sup>49</sup> D. M. Asner,<sup>37</sup> V. Aulchenko,<sup>1</sup> T. Aushev,<sup>14</sup> T. Aziz,<sup>44</sup> A. M. Bakich,<sup>43</sup> A. Bay,<sup>21</sup> V. Bhardwaj,<sup>29</sup> B. Bhuyan,<sup>10</sup> M. Bischofberger,<sup>29</sup> A. Bondar,<sup>1</sup> A. Bozek,<sup>32</sup> M. Bračko,<sup>24,15</sup> T. E. Browder,<sup>8</sup> P. Chen,<sup>31</sup> B. G. Cheon,<sup>7</sup> K. Chilikin,<sup>14</sup> R. Chistov,<sup>14</sup> K. Cho,<sup>18</sup> S.-K. Choi,<sup>6</sup> Y. Choi,<sup>42</sup> J. Dalseno,<sup>25,45</sup> M. Danilov,<sup>14</sup> Z. Doležal,<sup>2</sup> Z. Drásal,<sup>2</sup> S. Eidelman,<sup>1</sup> D. Epifanov,<sup>1</sup> J. E. Fast,<sup>37</sup> V. Gaur,<sup>44</sup> N. Gabyshev,<sup>1</sup> A. Garmash,<sup>1</sup> Y. M. Goh,<sup>7</sup> B. Golob,<sup>22,15</sup> J. Haba,<sup>9</sup> K. Hara,<sup>9</sup> T. Hara,<sup>9</sup> K. Hayasaka,<sup>28</sup> H. Hayashii,<sup>29</sup> T. Higuchi,<sup>9</sup> Y. Horii,<sup>28</sup> Y. Hoshi,<sup>47</sup> W.-S. Hou,<sup>31</sup> Y. B. Hsiung,<sup>31</sup> H. J. Hyun,<sup>20</sup> T. Iijima,<sup>28,27</sup> A. Ishikawa,<sup>48</sup> R. Itoh,<sup>9</sup> M. Iwabuchi,<sup>55</sup> Y. Iwasaki,<sup>9</sup> T. Iwashita,<sup>29</sup> T. Julius,<sup>26</sup> P. Kapusta,<sup>32</sup> N. Katayama,<sup>9</sup> T. Kawasaki,<sup>34</sup> H. Kichimi,<sup>9</sup> C. Kiesling,<sup>25</sup> H. J. Kim,<sup>20</sup> H. O. Kim,<sup>20</sup> J. B. Kim,<sup>19</sup> J. H. Kim,<sup>18</sup> K. T. Kim,<sup>19</sup> Y. J. Kim,<sup>18</sup> K. Kinoshita,<sup>3</sup> B. R. Ko,<sup>19</sup> S. Koblitz,<sup>25</sup> P. Kodyš,<sup>2</sup> S. Korpar,<sup>24,15</sup> P. Križan,<sup>22,15</sup> P. Krokovny,<sup>1</sup> T. Kuhr,<sup>17</sup> R. Kumar,<sup>38</sup> T. Kumita,<sup>51</sup> A. Kuzmin,<sup>1</sup> Y.-J. Kwon,<sup>55</sup> J. S. Lange,<sup>4</sup> S.-H. Lee,<sup>19</sup> J. Li,<sup>41</sup> Y. Li,<sup>53</sup> C. Liu,<sup>40</sup> Y. Liu,<sup>31</sup> Z. Q. Liu,<sup>11</sup> D. Liventsev,<sup>14</sup> R. Louvot,<sup>21</sup> D. Matvienko,<sup>1</sup> S. McOnie,<sup>43</sup> K. Miyabayashi,<sup>29</sup> H. Miyata,<sup>34</sup> Y. Miyazaki,<sup>27</sup> R. Mizuk,<sup>14</sup> G. B. Mohanty,<sup>44</sup> T. Mori,<sup>27</sup> N. Muramatsu,<sup>39</sup> E. Nakano,<sup>36</sup> M. Nakao,<sup>9</sup> H. Nakazawa,<sup>56</sup> S. Neubauer,<sup>17</sup> S. Nishida,<sup>9</sup> K. Nishimura,<sup>8</sup> O. Nitoh,<sup>52</sup> S. Ogawa,<sup>46</sup> T. Ohshima,<sup>27</sup> S. Okuno,<sup>16</sup> S. L. Olsen,<sup>41,8</sup> Y. Onuki,<sup>49</sup> H. Ozaki,<sup>9</sup> P. Pakhlov,<sup>14</sup> G. Pakhlova,<sup>14</sup> H. K. Park,<sup>20</sup> K. S. Park,<sup>42</sup> T. K. Pedlar,<sup>23</sup> R. Pestotnik,<sup>15</sup> M. Petrič,<sup>15</sup> L. E. Piilonen,<sup>53</sup> A. Poluektov,<sup>1</sup> M. Röhrken,<sup>17</sup> M. Rozanska,<sup>32</sup> H. Sahoo,<sup>8</sup> K. Sakai,<sup>9</sup> Y. Sakai,<sup>9</sup> T. Sanuki,<sup>48</sup> Y. Sato,<sup>48</sup> O. Schneider,<sup>21</sup> C. Schwanda,<sup>12</sup> A. J. Schwartz,<sup>3</sup> K. Senyo,<sup>54</sup> V. Shebalin,<sup>1</sup> C. P. Shen,<sup>27</sup> T.-A. Shibata,<sup>50</sup> J.-G. Shiu,<sup>31</sup> B. Shwartz,<sup>1</sup> A. Sibidanov,<sup>43</sup> F. Simon,<sup>25,45</sup> J. B. Singh,<sup>38</sup> P. Smerkol,<sup>15</sup> Y.-S. Sohn,<sup>55</sup> A. Sokolov,<sup>13</sup> E. Solovieva,<sup>14</sup> S. Stanič,<sup>35</sup> M. Starič,<sup>15</sup> M. Sumihama,<sup>5</sup> K. Sumisawa,<sup>9</sup> T. Sumiyoshi,<sup>51</sup> S. Tanaka,<sup>9</sup> G. Tatishvili,<sup>37</sup> Y. Teramoto,<sup>36</sup> I. Tikhomirov,<sup>14</sup> K. Trabelsi,<sup>9</sup> T. Tsuboyama,<sup>9</sup> M. Uchida,<sup>50</sup> S. Uehara,<sup>9</sup> T. Uglov,<sup>14</sup> Y. Unno,<sup>7</sup> S. Uno,<sup>9</sup> Y. Ushiroda,<sup>9</sup> S. E. Vahsen,<sup>8</sup> G. Varner,<sup>8</sup> K. E. Varvell,<sup>43</sup> A. Vinokurova,<sup>1</sup> V. Vorobyev,<sup>1</sup> C. H. Wang,<sup>30</sup> M.-Z. Wang,<sup>31</sup> P. Wang,<sup>11</sup> M. Watanabe,<sup>34</sup> Y. Watanabe,<sup>16</sup> K. M. Williams,<sup>53</sup> E. Won,<sup>19</sup> B. D. Yabsley,<sup>43</sup> H. Yamamoto,<sup>48</sup> Y. Yamashita,<sup>33</sup> M. Yamauchi,<sup>9</sup> Y. Yusa,<sup>34</sup> Z. P. Zhang,<sup>40</sup> V. Zhilich,<sup>1</sup> A. Zupanc,<sup>17</sup> and O. Zyukova<sup>1</sup>

(The Belle Collaboration)

<sup>1</sup>*Budker Institute of Nuclear Physics SB RAS and Novosibirsk State University, Novosibirsk 630090*<sup>2</sup>*Faculty of Mathematics and Physics, Charles University, Prague*<sup>3</sup>*University of Cincinnati, Cincinnati, Ohio 45221*<sup>4</sup>*Justus-Liebig-Universität Gießen, Gießen*<sup>5</sup>*Gifu University, Gifu*<sup>6</sup>*Gyeongsang National University, Chinju*<sup>7</sup>*Hanyang University, Seoul*<sup>8</sup>*University of Hawaii, Honolulu, Hawaii 96822*<sup>9</sup>*High Energy Accelerator Research Organization (KEK), Tsukuba*<sup>10</sup>*Indian Institute of Technology Guwahati, Guwahati*<sup>11</sup>*Institute of High Energy Physics, Chinese Academy of Sciences, Beijing*<sup>12</sup>*Institute of High Energy Physics, Vienna*<sup>13</sup>*Institute of High Energy Physics, Protvino*<sup>14</sup>*Institute for Theoretical and Experimental Physics, Moscow*<sup>15</sup>*J. Stefan Institute, Ljubljana*<sup>16</sup>*Kanagawa University, Yokohama*<sup>17</sup>*Institut für Experimentelle Kernphysik, Karlsruher Institut für Technologie, Karlsruhe*<sup>18</sup>*Korea Institute of Science and Technology Information, Daejeon*<sup>19</sup>*Korea University, Seoul*<sup>20</sup>*Kyungpook National University, Taegu*<sup>21</sup>*École Polytechnique Fédérale de Lausanne (EPFL), Lausanne*<sup>22</sup>*Faculty of Mathematics and Physics, University of Ljubljana, Ljubljana*<sup>23</sup>*Luther College, Decorah, Iowa 52101*<sup>24</sup>*University of Maribor, Maribor*<sup>25</sup>*Max-Planck-Institut für Physik, München*<sup>26</sup>*University of Melbourne, School of Physics, Victoria 3010*<sup>27</sup>*Graduate School of Science, Nagoya University, Nagoya*<sup>28</sup>*Kobayashi-Maskawa Institute, Nagoya University, Nagoya*<sup>29</sup>*Nara Women's University, Nara*<sup>30</sup>*National United University, Miao Li*<sup>31</sup>*Department of Physics, National Taiwan University, Taipei*<sup>32</sup>*H. Niewodniczanski Institute of Nuclear Physics, Krakow*

- <sup>33</sup>*Nippon Dental University, Niigata*  
<sup>34</sup>*Niigata University, Niigata*  
<sup>35</sup>*University of Nova Gorica, Nova Gorica*  
<sup>36</sup>*Osaka City University, Osaka*  
<sup>37</sup>*Pacific Northwest National Laboratory, Richland, Washington 99352*  
<sup>38</sup>*Panjab University, Chandigarh*  
<sup>39</sup>*Research Center for Nuclear Physics, Osaka University, Osaka*  
<sup>40</sup>*University of Science and Technology of China, Hefei*  
<sup>41</sup>*Seoul National University, Seoul*  
<sup>42</sup>*Sungkyunkwan University, Suwon*  
<sup>43</sup>*School of Physics, University of Sydney, NSW 2006*  
<sup>44</sup>*Tata Institute of Fundamental Research, Mumbai*  
<sup>45</sup>*Excellence Cluster Universe, Technische Universität München, Garching*  
<sup>46</sup>*Toho University, Funabashi*  
<sup>47</sup>*Tohoku Gakuin University, Tagajo*  
<sup>48</sup>*Tohoku University, Sendai*  
<sup>49</sup>*Department of Physics, University of Tokyo, Tokyo*  
<sup>50</sup>*Tokyo Institute of Technology, Tokyo*  
<sup>51</sup>*Tokyo Metropolitan University, Tokyo*  
<sup>52</sup>*Tokyo University of Agriculture and Technology, Tokyo*  
<sup>53</sup>*CNP, Virginia Polytechnic Institute and State University, Blacksburg, Virginia 24061*  
<sup>54</sup>*Yamagata University, Yamagata*  
<sup>55</sup>*Yonsei University, Seoul*  
<sup>56</sup>*National Central University, Chung-li*

We present a precise measurement of the  $CP$  violation parameter  $\sin 2\phi_1$  and the direct  $CP$  violation parameter  $\mathcal{A}_f$  using the final data sample of  $772 \times 10^6$   $B\bar{B}$  pairs collected at the  $\Upsilon(4S)$  resonance with the Belle detector at the KEKB asymmetric-energy  $e^+e^-$  collider. One neutral  $B$  meson is reconstructed in a  $J/\psi K_S^0$ ,  $\psi(2S)K_S^0$ ,  $\chi_{c1}K_S^0$  or  $J/\psi K_L^0$   $CP$ -eigenstate and its flavor is identified from the decay products of the accompanying  $B$  meson. From the distribution of proper time intervals between the two  $B$  decays, we obtain the following  $CP$  violation parameters:  $\sin 2\phi_1 = 0.667 \pm 0.023(\text{stat}) \pm 0.012(\text{syst})$  and  $\mathcal{A}_f = 0.006 \pm 0.016(\text{stat}) \pm 0.012(\text{syst})$ .

PACS numbers: 11.30.Er, 12.15.Hh, 13.25.Hw

In the standard model (SM),  $CP$  violation in the quark sector is described by the Kobayashi-Maskawa (KM) theory [1] in which the quark-mixing matrix has a single irreducible complex phase that gives rise to all  $CP$ -violating asymmetries. In the decay chain  $\Upsilon(4S) \rightarrow B^0\bar{B}^0 \rightarrow f_{CP}f_{\text{tag}}$ , where one of the  $B$  mesons decays at time  $t_{CP}$  to a  $CP$ -eigenstate  $f_{CP}$  and the other  $B$  meson decays at time  $t_{\text{tag}}$  to a final state  $f_{\text{tag}}$  that distinguishes between  $B^0$  and  $\bar{B}^0$ , the decay rate has a time dependence in the  $\Upsilon(4S)$  rest frame [2] given by

$$\mathcal{P}(\Delta t) = \frac{e^{-|\Delta t|/\tau_{B^0}}}{4\tau_{B^0}} \left\{ 1 + q \left[ \mathcal{S}_f \sin(\Delta m_d \Delta t) + \mathcal{A}_f \cos(\Delta m_d \Delta t) \right] \right\}. \quad (1)$$

Here  $\mathcal{S}_f$  and  $\mathcal{A}_f$  are  $CP$  violation parameters,  $\tau_{B^0}$  is the  $B^0$  lifetime,  $\Delta m_d$  is the mass difference between the two neutral  $B$  mass eigenstates,  $\Delta t \equiv t_{CP} - t_{\text{tag}}$ , and the  $b$ -flavor charge  $q = +1$  ( $-1$ ) when the tagging  $B$  meson is a  $B^0$  ( $\bar{B}^0$ ). With very small theoretical uncertainty [2], the SM predicts  $\mathcal{S}_f = -\xi_f \sin 2\phi_1$  and  $\mathcal{A}_f = 0$  for the  $b \rightarrow c\bar{c}s$  transition, where  $\xi_f = +1$  ( $-1$ ) corresponds to  $CP$ -even ( $-$ odd) final states and  $\phi_1$  is an interior angle of the KM unitarity triangle, defined as  $\phi_1 \equiv \arg[-V_{cd}V_{cb}^*/V_{td}V_{tb}^*]$  [3]. The BaBar and Belle

collaborations have published several determinations of  $\sin 2\phi_1$  since the first observation [4, 5]; previous results used  $465 \times 10^6$  [6] and  $535 \times 10^6$  [7]  $B\bar{B}$  pairs, respectively.

With recently available experimental results, not only  $\sin 2\phi_1$  but also other measurements of the sides of the unitarity triangle and other  $CP$  violation measurements make it possible to test the consistency of the KM scheme. The indirect determination of the angle  $\phi_1$  deviates by  $2.7\sigma$  from the current world average for the direct determination of  $\sin 2\phi_1$  [8]. Equivalently, the  $B^\pm \rightarrow \tau^\pm \nu_\tau$  branching fraction and the resulting value of  $|V_{ub}|$  differ by  $2.8\sigma$  from the prediction of the global fit [8], where the  $\sin 2\phi_1$  value gives the most stringent constraint on the indirect measurement. Furthermore, time-dependent  $CP$  violation in the neutral  $B$  meson decays mediated by flavor-changing  $b \rightarrow s$  transitions may deviate from  $CP$  violation in the  $b \rightarrow c\bar{c}s$  case because of possible additional quantum loops [9]. To clarify whether new physics contributes to  $CP$ -violating phenomena or  $B^\pm \rightarrow \tau^\pm \nu_\tau$  decays, it is very important to determine  $\sin 2\phi_1$ , the SM reference, as precisely as possible.

In this Letter, we describe the final Belle measurement of  $\sin 2\phi_1$  and  $\mathcal{A}_f$  in  $b \rightarrow c\bar{c}s$  induced  $B$  decays to  $f_{CP}$ . The  $B$  decays to the  $CP$ -odd eigenstates,  $f_{CP} = J/\psi K_S^0$ ,  $\psi(2S)K_S^0$  and  $\chi_{c1}K_S^0$ , and the  $CP$ -even eigenstate,  $f_{CP} = J/\psi K_L^0$ , are reconstructed using  $772 \times 10^6$

$B\bar{B}$  pairs, the entire data sample accumulated on the  $\Upsilon(4S)$  resonance with the Belle detector [10] at the KEKB asymmetric-energy  $e^+e^-$  collider [11]. Two inner detector configurations were used. A 2.0 cm radius beampipe and a 3-layer silicon vertex detector (SVD) were used for the first data sample that contains  $152 \times 10^6$   $B\bar{B}$  pairs. The remaining  $620 \times 10^6$   $B\bar{B}$  pairs were accumulated with a 1.5 cm radius beampipe, a 4-layer silicon vertex detector and a small-cell inner drift chamber. The latter data sample has been recently reprocessed using a new charged track reconstruction algorithm, which significantly increased the reconstruction efficiency for the  $B^0 \rightarrow (c\bar{c})K_S^0$  decay modes. In particular, the gain for the  $B^0 \rightarrow J/\psi K_S^0$  decay mode is 18%.

The  $\Upsilon(4S)$  is produced with a Lorentz boost of  $\beta\gamma = 0.425$  nearly along the  $z$ -axis, which is antiparallel to the positron beam direction. Since the  $B^0$  and  $\bar{B}^0$  mesons are approximately at rest in the  $\Upsilon(4S)$  center-of-mass system (CM),  $\Delta t$  can be determined from the displacement in  $z$  between the  $f_{CP}$  and  $f_{\text{tag}}$  decay vertices:  $\Delta t \simeq (z_{CP} - z_{\text{tag}})/(\beta\gamma c) \equiv \Delta z/(\beta\gamma c)$ .

Charged tracks reconstructed in the central drift chamber (CDC), except for tracks from  $K_S^0 \rightarrow \pi^+\pi^-$  decays, are required to originate from the interaction point (IP). We distinguish charged kaons from pions based on a kaon (pion) likelihood  $\mathcal{L}_{K(\pi)}$  derived from the time-of-flight scintillation counters, aerogel threshold Cherenkov counters (ACC), and  $dE/dx$  measurements in the CDC. Electron identification is based on the ratio of the electromagnetic calorimeter (ECL) cluster energy to the particle momentum as well as a combination of  $dE/dx$  measurements in the CDC, the ACC response, and the position and shape of the electromagnetic shower. Muons are identified by track penetration depth and hit scatter in the muon detector (KLM). Photons are identified as isolated ECL clusters that are not matched to any charged track.

For the  $J/\psi K_S^0$ ,  $J/\psi K_L^0$  and  $\psi(2S)K_S^0$  modes, event selection is the same as in our previous analyses [7, 12], where  $J/\psi$  mesons are reconstructed via their decays to  $\ell^+\ell^-$  ( $\ell = e, \mu$ ) and the  $\psi(2S)$  mesons to  $\ell^+\ell^-$  or  $J/\psi\pi^+\pi^-$ . For the modes  $J/\psi K_L^0$  and  $\chi_{c1}K_S^0$ , in which the  $\chi_{c1}$  is reconstructed in the  $J/\psi\gamma$  final state, both  $J/\psi$  daughter tracks must be positively identified as leptons, whereas for the  $J/\psi K_S^0$  and  $\psi(2S)K_S^0$  modes, at least one daughter must satisfy this requirement. Any other track having an ECL energy deposit consistent with a minimum ionizing particle is accepted as a muon candidate and any track satisfying either the  $dE/dx$  or the ECL shower energy requirements is retained as an electron candidate. For  $J/\psi \rightarrow e^+e^-$  decays, the  $e^\pm$  charmonium daughters are combined with photons found within 50 mrad of the  $e^+$  or  $e^-$  direction in order to account partially for final-state radiation and bremsstrahlung. In order to accommodate the remaining radiative tails, an asymmetric invariant mass requirement is used to select  $J/\psi$  and  $\psi(2S)$  decays in dilepton modes,  $-150 \text{ MeV}/c^2 < M_{e^+e^-} - M_\psi < 36 \text{ MeV}/c^2$

and  $-60 \text{ MeV}/c^2 < M_{\mu^+\mu^-} - M_\psi < 36 \text{ MeV}/c^2$ , where  $M_\psi$  denotes either the nominal  $J/\psi$  or  $\psi(2S)$  mass. For  $\psi(2S) \rightarrow J/\psi\pi^+\pi^-$  candidates, we require a mass difference of  $580 \text{ MeV}/c^2 < M_{\ell^+\ell^-\pi^+\pi^-} - M_{\ell^+\ell^-} < 600 \text{ MeV}/c^2$ , and  $\chi_{c1} \rightarrow J/\psi\gamma$  candidates are required to have a mass difference of  $385.0 \text{ MeV}/c^2 < M_{\ell^+\ell^-\gamma} - M_{\ell^+\ell^-} < 430.5 \text{ MeV}/c^2$ . For each charmonium candidate, vertex-constrained and mass-constrained fits are applied to improve its momentum resolution.

Candidate  $K_S^0 \rightarrow \pi^+\pi^-$  decays are selected by requirements on their invariant mass, flight length and consistency between the  $K_S^0$  momentum direction and vertex position. Candidate  $K_L^0$  mesons are selected from ECL and/or KLM hit patterns that are consistent with the presence of a shower induced by a  $K_L^0$  meson. The centroid of the  $K_L^0$  candidate shower is required to be within a  $45^\circ$  cone centered on the  $K_L^0$  direction calculated from the two-body  $B$  decay kinematics and the momentum of the reconstructed  $J/\psi$  meson.

For  $B \rightarrow f_{CP}$  candidate reconstruction in modes other than  $J/\psi K_L^0$ ,  $B$  candidates are identified by two kinematic variables: the energy difference  $\Delta E \equiv E_B^* - E_{\text{beam}}^*$  and the beam-energy constrained mass  $M_{\text{bc}} \equiv \sqrt{(E_{\text{beam}}^*)^2 - (p_B^*)^2}$ , where  $E_{\text{beam}}^*$  is the CM beam energy, and  $E_B^*$  ( $p_B^*$ ) is the CM energy (momentum) of the reconstructed  $B$  candidate. The  $B^0 \rightarrow J/\psi K_L^0$  candidates are identified by the value of  $p_B^*$  calculated using a two-body decay kinematic assumption.

The  $b$ -flavor of the accompanying  $B$  meson is identified from inclusive properties of particles that are not associated with the reconstructed  $B^0 \rightarrow f_{CP}$  decay [13]. The tagging information is represented by two parameters, the  $b$ -flavor charge  $q$  and purity  $r$ . The parameter  $r$  is an event-by-event, MC-determined flavor-tagging dilution factor that ranges from  $r = 0$  for no flavor discrimination to  $r = 1$  for unambiguous flavor assignment. The data are sorted into seven intervals of  $r$ . For events with  $r > 0.1$ , the wrong tag fractions for six  $r$  intervals,  $w_l$  ( $l = 1, 6$ ), and their differences between  $B^0$  and  $\bar{B}^0$  decays,  $\Delta w_l$ , are determined from semileptonic and hadronic  $b \rightarrow c$  decays [12, 14]. If  $r \leq 0.1$ , the wrong tag fraction is set to 0.5, and therefore the tagging information is not used. The total effective tagging efficiency,  $\Sigma(f_l \times (1 - 2w_l)^2)$ , is determined to be  $0.298 \pm 0.004$ , where  $f_l$  is the fraction of events in the category  $l$ .

The vertex position for the  $f_{CP}$  decay is reconstructed using  $J/\psi$  or  $\psi(2S)$  daughter tracks that have a minimum number of SVD hits, while the  $f_{\text{tag}}$  vertex is determined from well-reconstructed tracks that are not assigned to  $f_{CP}$  [14]. A constraint on the IP profile in the plane perpendicular to the  $z$ -axis is used with the selected tracks. With this procedure, we are able to determine a vertex even in the case where only one track has sufficient associated SVD hits. The fractions of the single track vertices for  $f_{CP}$  and  $f_{\text{tag}}$  are about 12% and 23%, respectively.

For a single track vertex, the estimated error of the  $z$  coordinate,  $\sigma_z$ , is the indicator of the vertex fit quality and is required to be less than 500  $\mu\text{m}$ . On the

other hand, a vertex reconstructed using two or more tracks is characterized by a more robust goodness-of-fit indicator. In the previous analysis [7], the value of  $\chi^2$  of the vertex calculated solely along the  $z$  direction was used. This is now replaced by  $h$ , the value of  $\chi^2$  in three-dimensional space calculated using the charged tracks *without* using the interaction-region profile's constraint [15]. A detailed MC study indicates that  $h$  is a superior indicator of the vertex goodness-of-fit because it is less sensitive to the specific  $B$  decay mode; in particular,  $h$  shows a smaller mode dependence for the vertices reconstructed from  $B \rightarrow J/\psi X$  and  $B \rightarrow D^{(*)}X$  decays, which are used as control samples to determine the vertex resolution parameters. In the multiple-track vertex case,  $h < 50$  and  $\sigma_z < 200 \mu\text{m}$  are required. For candidate events in which both  $B$  vertices are reconstructed, we retain only those events where the  $B$  vertices satisfy  $|\Delta t| < 70 \text{ ps}$  for further analysis.

For the candidate events in which both flavor tagging and vertex reconstruction succeed, the signal yield and purity for each mode are obtained from an unbinned maximum-likelihood fit to the two-dimensional  $\Delta E - M_{bc}$  distribution for  $f_{CP}$  modes with a  $K_S^0$  meson, and to the  $p_B^*$  distribution for  $J/\psi K_L^0$ . The background mainly comes from  $B\bar{B}$  events in which one of the  $B$  mesons decays into a final state containing a correctly reconstructed  $J/\psi$ , i.e., the  $B \rightarrow J/\psi X$  process. In order to determine this background distribution, a  $B \rightarrow J/\psi X$  MC sample corresponding to 100 times the integrated luminosity of data is used. An estimate of other combinatorial backgrounds is obtained from the  $M_{\ell+\ell^-}$  sideband. For  $CP$ -odd modes, the signal distribution is modeled with a Gaussian function in  $M_{bc}$  and a double Gaussian function in  $\Delta E$ . The fits to determine signal yields for these modes are performed in the region  $5.2 \text{ GeV}/c^2 < M_{bc} < 5.3 \text{ GeV}/c^2$  and  $-0.1 \text{ GeV} < \Delta E < 0.2 \text{ GeV}$ . The  $p_B^*$  signal shape for  $J/\psi K_L^0$  is determined from MC events. The requirement  $p_B^* < 2.0 \text{ GeV}/c$  is used in the fit to estimate the signal yield as well as the contribution of three categories of background: those with a real (those that are correctly reconstructed)  $J/\psi$  and a real  $K_L^0$ , those with a real  $J/\psi$  and a fake  $K_L^0$  (those that are incorrectly reconstructed from electronic noise or electro-magnetic showers), and events with a fake  $J/\psi$  (those that are background combinations). The  $M_{bc}$  distribution for a stringent  $\Delta E$  requirement ( $|\Delta E| < 40 \text{ MeV}$  for  $J/\psi K_S^0$ ,  $|\Delta E| < 30 \text{ MeV}$  for  $\psi(2S)K_S^0$  and  $|\Delta E| < 25 \text{ MeV}$  for  $\chi_{c1}K_S^0$ ) as well as the  $p_B^*$  distribution for  $J/\psi K_L^0$  candidates are shown in Fig. 1. We require  $5.27 \text{ GeV}/c^2 < M_{bc} < 5.29 \text{ GeV}/c^2$  for  $f_{CP}$  modes with a  $K_S^0$  and  $0.20 \text{ GeV}/c < p_B^* < 0.45 \text{ GeV}/c$  for  $J/\psi K_L^0$  for the fit to the  $CP$  violation parameters. For the candidates passing all the criteria mentioned above, the signal yield and purity are estimated for each  $CP$ -eigenstate and listed in Table I.

We determine  $\mathcal{S}_f$  and  $\mathcal{A}_f$  for each mode by performing an unbinned maximum-likelihood fit to the observed  $\Delta t$  distribution. The probability density function (PDF)

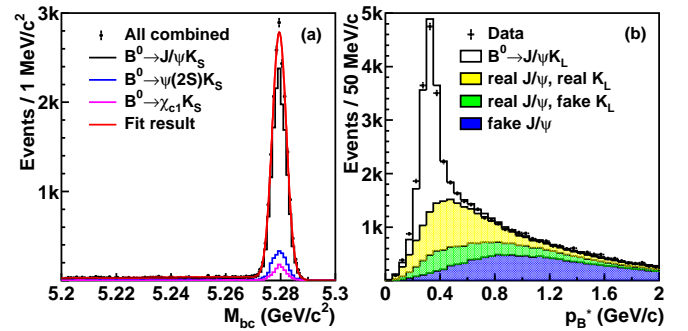


FIG. 1: (color online). (a)  $M_{bc}$  distribution within the  $\Delta E$  signal region for  $B^0 \rightarrow J/\psi K_S^0$  (black),  $\psi(2S)K_S^0$  (blue), and  $\chi_{c1}K_S^0$  (magenta); the superimposed curve (red) shows the combined fit result for all these modes. (b)  $p_B^*$  distribution of  $B^0 \rightarrow J/\psi K_L^0$  candidates with the results of the fit separately indicated as signal (open histogram), background with a real  $J/\psi$  and real  $K_L^0$ 's (yellow), with a real  $J/\psi$  and a fake  $K_L^0$  candidate (green), and with a fake  $J/\psi$  (blue).

TABLE I:  $CP$  eigenvalue ( $\xi_f$ ), signal yield ( $N_{\text{sig}}$ ) and purity for each  $B^0 \rightarrow f_{CP}$  mode.

Decay mode	$\xi_f$	$N_{\text{sig}}$	Purity (%)
$J/\psi K_S^0$	-1	$12649 \pm 114$	97
$\psi(2S)(\ell^+\ell^-)K_S^0$	-1	$904 \pm 31$	92
$\psi(2S)(J/\psi\pi^+\pi^-)K_S^0$	-1	$1067 \pm 33$	90
$\chi_{c1}K_S^0$	-1	$940 \pm 33$	86
$J/\psi K_L^0$	+1	$10040 \pm 154$	63

for the signal distribution,  $\mathcal{P}_{\text{sig}}(\Delta t; \mathcal{S}_f, \mathcal{A}_f, q, w_l, \Delta w_l)$ , is given by Eq. (1), fixing  $\tau_{B^0}$  and  $\Delta m_d$  at their world average values [16] and including modifications to take the effect of incorrect flavor assignment (parameterized by  $w_l$  and  $\Delta w_l$ ) into account. The distribution is convolved with the proper-time interval resolution function,  $R_{\text{sig}}(\Delta t)$ , formed by convolving four components: the detector resolutions for  $z_{CP}$  and  $z_{\text{tag}}$ , the shift of the  $z_{\text{tag}}$  vertex position due to secondary tracks from charmed particle decays, and the kinematic approximation that the  $B$  mesons are at rest in the CM frame [17]. Because we now use  $h$  to characterize the vertex goodness-of-fit, each of these resolution function components in Ref. [17] is reformulated as a function of  $h$  and  $\sigma_z$ .

Using the  $M_{bc}$  sideband events, the background PDF,  $\mathcal{P}_{\text{bkg}}(\Delta t)$ , for each of the  $CP$ -odd modes is modeled as a sum of exponential and prompt components, and is convolved with  $R_{\text{bkg}}(\Delta t)$  expressed as a double Gaussian function. In the  $J/\psi K_L^0$  mode, there are  $CP$  violating modes among the  $B \rightarrow J/\psi X$  backgrounds, which are included in the background PDF. The  $\Delta t$  PDFs for the remaining  $B \rightarrow J/\psi X$  and other combinatorial backgrounds are estimated from the corresponding large MC sample and  $M_{\ell+\ell^-}$  sideband events, respectively. The construction of these PDFs follows the same procedure

as in our previous analyses [7, 12].

We determine the following likelihood for the  $i$ -th event:

$$P_i = (1 - f_{\text{ol}}) \sum_k f_k \int [\mathcal{P}_k(\Delta t') R_k(\Delta t_i - \Delta t')] d(\Delta t') + f_{\text{ol}} P_{\text{ol}}(\Delta t_i), \quad (2)$$

where the index  $k$  labels each signal or background component. The fraction  $f_k$  depends on the  $r$  region and is calculated on an event-by-event basis as a function of  $\Delta E$  and  $M_{\text{bc}}$  for the  $CP$ -odd modes and  $p_B^*$  for the  $CP$ -even mode. The term  $P_{\text{ol}}(\Delta t)$  is a broad Gaussian function that represents an outlier component  $f_{\text{ol}}$ , which has a fractional normalization of order 0.5% [17]. The only free parameters in the fits are  $\mathcal{S}_f$  and  $\mathcal{A}_f$ , which are determined by maximizing the likelihood function  $L = \prod_i P_i(\Delta t_i; \mathcal{S}_f, \mathcal{A}_f)$ . This likelihood is maximized for each  $f_{CP}$  mode individually, as well as for all modes combined taking into account their  $CP$ -eigenstate values; the results are shown in Table II. Figure 2 shows the  $\Delta t$  distributions and asymmetries for good tag quality ( $r > 0.5$ ) events. We define the background-subtracted asymmetry in each  $\Delta t$  bin by  $(N_+ - N_-)/(N_+ + N_-)$ , where  $N_+(N_-)$  is the signal yield with  $q = +1(-1)$ .

TABLE II:  $CP$  violation parameters for each  $B^0 \rightarrow f_{CP}$  mode and from the simultaneous fit for all modes together. The first and second errors are statistical and systematic uncertainties, respectively.

Decay mode	$\sin 2\phi_1 \equiv -\xi_f \mathcal{S}_f$	$\mathcal{A}_f$
$J/\psi K_S^0$	$+0.670 \pm 0.029 \pm 0.013$	$-0.015 \pm 0.021^{+0.045}_{-0.023}$
$\psi(2S) K_S^0$	$+0.738 \pm 0.079 \pm 0.036$	$+0.104 \pm 0.055^{+0.047}_{-0.027}$
$\chi_{c1} K_S^0$	$+0.640 \pm 0.117 \pm 0.040$	$-0.017 \pm 0.083^{+0.046}_{-0.026}$
$J/\psi K_L^0$	$+0.642 \pm 0.047 \pm 0.021$	$+0.019 \pm 0.026^{+0.017}_{-0.041}$
All modes	$+0.667 \pm 0.023 \pm 0.012$	$+0.006 \pm 0.016 \pm 0.012$

Uncertainties originating from the vertex reconstruction algorithm are a significant part of the systematic error for both  $\sin 2\phi_1$  and  $\mathcal{A}_f$ . These uncertainties are reduced by almost a factor of two compared to the previous analysis [7] by using  $h$  for the vertex-reconstruction goodness-of-fit parameter, as described above. In particular, the effect of the vertex quality cut is estimated by changing the requirement to either  $h < 25$  or  $h < 100$ ; the systematic error due to the IP constraint in the vertex reconstruction is estimated by varying the IP profile size in the plane perpendicular to the  $z$ -axis; the effect of the criterion for the selection of tracks used in the  $f_{\text{tag}}$  vertex is estimated by changing the requirement on the distance of closest approach with respect to the reconstructed vertex by  $\pm 100 \mu\text{m}$  from the nominal maximum value of  $500 \mu\text{m}$ . Systematic errors due to imperfect SVD alignment are estimated from MC samples that have artificial misalignment effects. Small biases in the  $\Delta z$  measurement are

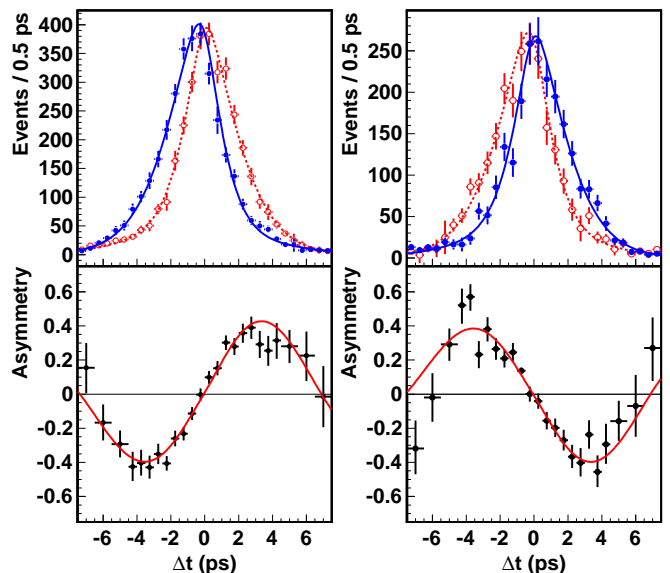


FIG. 2: (color online) The background-subtracted  $\Delta t$  distribution (top) for  $q = +1$  (red) and  $q = -1$  (blue) events and asymmetry (bottom) for good tag quality ( $r > 0.5$ ) events for all  $CP$ -odd modes combined (left) and the  $CP$ -even mode (right).

TABLE III: Systematic errors in  $\mathcal{S}_f$  and  $\mathcal{A}_f$  in each  $f_{CP}$  mode and for the sum of all modes.

	$J/\psi K_S^0$	$\psi(2S) K_S^0$	$\chi_{c1} K_S^0$	$J/\psi K_L^0$	All	
Vertexing	$\mathcal{S}_f$	$\pm 0.008$	$\pm 0.031$	$\pm 0.025$	$\pm 0.011$	$\pm 0.007$
	$\mathcal{A}_f$	$\pm 0.022$	$\pm 0.026$	$\pm 0.021$	$\pm 0.015$	$\pm 0.007$
$\Delta t$ resolution	$\mathcal{S}_f$	$\pm 0.007$	$\pm 0.007$	$\pm 0.005$	$\pm 0.007$	$\pm 0.007$
	$\mathcal{A}_f$	$\pm 0.004$	$\pm 0.003$	$\pm 0.004$	$\pm 0.003$	$\pm 0.001$
Tag-side interference	$\mathcal{S}_f$	$\pm 0.002$	$\pm 0.002$	$\pm 0.002$	$\pm 0.001$	$\pm 0.001$
	$\mathcal{A}_f$	$^{+0.038}_{-0.000}$	$^{+0.038}_{-0.000}$	$^{+0.038}_{-0.000}$	$^{+0.000}_{-0.037}$	$\pm 0.008$
Flavor tagging	$\mathcal{S}_f$	$\pm 0.003$	$\pm 0.003$	$\pm 0.004$	$\pm 0.003$	$\pm 0.004$
	$\mathcal{A}_f$	$\pm 0.003$	$\pm 0.003$	$\pm 0.003$	$\pm 0.003$	$\pm 0.003$
Possible fit bias	$\mathcal{S}_f$	$\pm 0.004$	$\pm 0.004$	$\pm 0.004$	$\pm 0.004$	$\pm 0.004$
	$\mathcal{A}_f$	$\pm 0.005$	$\pm 0.005$	$\pm 0.005$	$\pm 0.005$	$\pm 0.005$
Signal fraction	$\mathcal{S}_f$	$\pm 0.004$	$\pm 0.016$	$< 0.001$	$\pm 0.016$	$\pm 0.004$
	$\mathcal{A}_f$	$\pm 0.002$	$\pm 0.006$	$< 0.001$	$\pm 0.006$	$\pm 0.002$
Background $\Delta t$ PDFs	$\mathcal{S}_f$	$< 0.001$	$\pm 0.002$	$\pm 0.030$	$\pm 0.002$	$\pm 0.001$
	$\mathcal{A}_f$	$< 0.001$	$< 0.001$	$\pm 0.014$	$< 0.001$	$< 0.001$
Physics parameters	$\mathcal{S}_f$	$\pm 0.001$	$\pm 0.001$	$\pm 0.001$	$\pm 0.001$	$\pm 0.001$
	$\mathcal{A}_f$	$< 0.001$	$< 0.001$	$\pm 0.001$	$< 0.001$	$< 0.001$
Total	$\mathcal{S}_f$	$\pm 0.013$	$\pm 0.036$	$\pm 0.040$	$\pm 0.021$	$\pm 0.012$
	$\mathcal{A}_f$	$^{+0.045}_{-0.023}$	$^{+0.047}_{-0.027}$	$^{+0.046}_{-0.026}$	$^{+0.017}_{-0.041}$	$\pm 0.012$

observed in  $e^+e^- \rightarrow \mu^+\mu^-$  and other control samples: to account for these, a special correction function is applied and the variation with respect to the nominal results is included as a systematic error. We also vary the  $|\Delta t|$  range by  $\pm 30$  ps to estimate the systematic uncertainty due to the  $|\Delta t|$  fit range. The vertex resolution function

is another major source of  $\sin 2\phi_1$  and  $\mathcal{A}_f$  uncertainty. This effect is estimated by varying each resolution function parameter obtained from data (MC) by  $\pm 1\sigma$  ( $\pm 2\sigma$ ) and repeating the fit to add each variation in quadrature. The uncertainty in the estimated errors of the parameters of reconstructed charged tracks is also taken into account. The largest contribution to the systematic uncertainty in  $\mathcal{A}_f$  is the effect of the tag-side interference (TSI), which is described in detail in [18]. Since the effect of TSI has opposite sign for different  $CP$ -eigenstates, there is a partial cancellation in the combined result. Hence the combined TSI systematic is smaller than the systematic in each individual mode. Systematic errors due to uncertainties in the wrong-tag fractions are studied by varying the wrong-tag fraction individually in each  $r$  region. A possible fit bias is examined by fitting a large number of MC events. Other contributions come from uncertainties in the signal fractions, the background  $\Delta t$  distribution,  $\tau_{B^0}$  and  $\Delta m_d$ . Each contribution is summarized in Table III. We add them in quadrature to obtain the total systematic uncertainty.

In summary, we present the final  $\sin 2\phi_1$  measurement using the entire Belle  $\Upsilon(4S)$  data sample con-

taining  $772 \times 10^6$   $B\bar{B}$  pairs. We have reconstructed  $b \rightarrow c\bar{c}s$  induced  $B$  meson decays in three  $CP$ -odd modes ( $J/\psi K_S^0$ ,  $\psi(2S)K_S^0$ , and  $\chi_{c1}K_S^0$ ) and one  $CP$ -even mode ( $J/\psi K_L^0$ ). The fit, using common  $CP$ -sensitive parameters for all four modes, yields the values  $\sin 2\phi_1 = 0.667 \pm 0.023(\text{stat}) \pm 0.012(\text{syst})$  and  $\mathcal{A}_f = 0.006 \pm 0.016(\text{stat}) \pm 0.012(\text{syst})$ . The results are consistent with previous measurements [6, 7]. These are the most precise determination of these parameters and solidify the SM reference value used to test for evidence of new physics beyond the SM.

We thank the KEKB group for excellent operation of the accelerator; the KEK cryogenics group for efficient solenoid operations; and the KEK computer group, the NII, and PNNL/EMSL for valuable computing and SINET4 network support. We acknowledge support from MEXT, JSPS and Nagoya's TLPRC (Japan); ARC and DIISR (Australia); NSFC (China); MSMT (Czechia); DST (India); INFN (Italy); MEST, NRF, GSDC of KISTI, and WCU (Korea); MNiSW (Poland); MES and RFAAE (Russia); ARRS (Slovenia); SNSF (Switzerland); NSC and MOE (Taiwan); and DOE and NSF (USA).

- 
- [1] M. Kobayashi and T. Maskawa, *Prog. Theor. Phys.* **49**, 652 (1973).
- [2] A. B. Carter and A. I. Sanda, *Phys. Rev. D* **23**, 1567 (1981); I. I. Bigi and A. I. Sanda, *Nucl. Phys. B* **193**, 85 (1981).
- [3] Another naming convention  $\beta(\equiv \phi_1)$  is also used in the literature.
- [4] B. Aubert *et al.* (BaBar Collaboration), *Phys. Rev. Lett.* **87**, 091801 (2001).
- [5] K. Abe *et al.* (Belle Collaboration), *Phys. Rev. Lett.* **87**, 091802 (2001).
- [6] B. Aubert *et al.* (BaBar Collaboration), *Phys. Rev. D* **79**, 072009 (2009).
- [7] K. F. Chen *et al.* (Belle Collaboration), *Phys. Rev. Lett.* **98**, 031802 (2007).
- [8] J. Charles *et al.* (CKMfitter group), *Phys. Rev. D* **84**, 033005 (2011).
- [9] Y. Grossman and M. P. Worah, *Phys. Lett. B* **395**, 241 (1997); D. London and A. Soni, *Phys. Lett. B* **407**, 61 (1997); T. Moroi, *Phys. Lett. B* **493**, 366 (2000); D. Chang, A. Masiero and H. Murayama, *Phys. Rev. D* **67**, 075013 (2003); S. Baek, T. Goto, Y. Okada and K.I. Okumura, *Phys. Rev. D* **64**, 095001 (2001).
- [10] A. Abashian *et al.* (Belle Collaboration), *Nucl. Instrum. Methods Phys. Res., Sect. A* **479**, 117 (2002).
- [11] S. Kurokawa and E. Kikutani, *Nucl. Instrum. Methods Phys. Res., Sect. A* **499**, 1 (2003), and other papers included in this volume.
- [12] K. Abe *et al.* (Belle Collaboration), *Phys. Rev. D* **71**, 072003 (2005); H. Sahoo *et al.* (Belle Collaboration), *Phys. Rev. D* **77**, 091103 (2008).
- [13] H. Kakuno *et al.*, *Nucl. Instrum. Methods Phys. Res., Sect. A* **533**, 516 (2004).
- [14] K. F. Chen *et al.* (Belle Collaboration), *Phys. Rev. D* **72**, 012004 (2005).
- [15] Details of the vertex fit and the parameterization of the resolution function are given in an accompanying *Phys. Rev. D* paper (in preparation).
- [16] K. Nakamura *et al.* (Particle Data Group), *J. Phys. G* **37**, 075021 (2010).
- [17] H. Tajima *et al.*, *Nucl. Instrum. Methods Phys. Res., Sect. A* **533**, 370 (2004).
- [18] O. Long, M. Baak, R.N. Cahn and D. Kirkby, *Phys. Rev. D* **68**, 034010 (2003).